Arabian Journal of Chemistry (2020) **13**, 1415–1428

King Saud University

Arabian Journal of Chemistry

www.ksu.edu.sa
www.sciencedirect.com

ORIGINAL ARTICLE

Carnivorous plants used for green synthesis of silver nanoparticles with broad-spectrum antimicrobial activity

Rafal Banasiuk [a], Marta Krychowiak [a], Daria Swigon [a], Wojciech Tomaszewicz [a], Angelika Michalak [a], Agnieszka Chylewska [b], Magdalena Ziabka [c], Marcin Lapinski [d], Barbara Koscielska [d], Magdalena Narajczyk [e], Aleksandra Krolicka [a,*]

[a] *University of Gdansk, Intercollegiate Faculty of Biotechnology University of Gdansk and Medical University of Gdansk, Laboratory of Biologically Active Compounds, Abrahama 58, 80-307 Gdansk, Poland*
[b] *University of Gdansk, Faculty of Chemistry, Laboratory of Intermolecular Interactions, W. Stwosza 63, 80-308 Gdansk, Poland*
[c] *AGH-University of Science and Technology, Faculty of Materials Science and Ceramics, Department of Ceramics and Refractories, Al. A. Mickiewicza 30, 30-059 Krakow, Poland*
[d] *Gdansk University of Technology, Faculty of Applied Physics and Mathematics, Department of Solid State Physics, G. Narutowicza 11/12, 80-233 Gdansk, Poland*
[e] *University of Gdansk, Faculty of Biology, Laboratory of Electron Microscopy, Wita Stwosza 59, 80-308 Gdansk, Poland*

Received 14 June 2017; accepted 19 November 2017
Available online 6 December 2017

KEYWORDS

Candida albicans;
Drosera;
Dionaea;
Energy efficiency;
Plant pathogens;
Staphylococcus aureus;
Pseudomonas aeruginosa

Abstract In this study, we exploit the anti-oxidative potential of four carnivorous plants to produce uniform and biologically active silver nanoparticles. The use of polyvinylpyrrolidone promoted synthesis of quasi-spherical nanoparticles characterized by stability and high uniformity. Their activity was tested against three human pathogens and three species of plant pathogenic bacteria. The study demonstrates the influence of synthesis method (microwave irradiation or heat radiation) and plant extract composition on nanoparticle activity. The total anti-oxidative potential of the plant extract, as well as the applied method of silver ions reduction proved to be crucial for antimicrobial activity. The highest minimal bactericidal concentration (mean value = 10 μg/mL) was obtained for silver nanoparticles synthesized with the use of water extract from *Dionaea muscipula* tissue.

* Corresponding author.
E-mail address: aleksandra.krolicka@biotech.ug.edu.pl (A. Krolicka).
Peer review under responsibility of King Saud University.

Production and hosting by Elsevier

https://doi.org/10.1016/j.arabjc.2017.11.013
1878-5352

1. Introduction

Nanotechnology is a fast-growing field of science due to the increasing interest in nanostructures (Eckhardt et al., 2013). Nanoparticles are structures with at least one dimension under 100 nm and have high surface to mass ratio. This gives them unique properties that their macroscopic counterparts do not possess and enables their use for instance in: electronics (Lee et al., 2008), bioremediation (Cropek et al., 2008), biological markers (Edelstein et al., 2000), catalysts (Astruc et al., 2005), antimicrobials (Lara et al., 2011). The list of potential applications is constantly growing as a number of products containing nanostructures are commercially available. Increasing trend of NPs commercialization demands safer, reproducible and inexpensive synthesis methods. The most popular type of nanomaterials is silver nanoparticles (AgNPs). Because of their antimicrobial properties, they found various applications in products for personal hygiene, cleaning and disinfection, building materials, medical products, textiles, and even food processing (Tran et al., 2013). In recent years many studies have been conducted to test nanoparticles' toxicity towards living organisms. Those reports suggested that silver nanoparticles show high cytotoxicity towards both human and bacterial cells (Foldbjerg et al., 2011, Lubick, 2008). However, a later research indicated that the toxic effect is the result of ion dissolution from AgNPs over time (Kittler et al., 2010) and it points that only Ag^+ ions contribute to nanosilver toxicity (Beer et al., 2012).

Silver nanoparticles are produced mainly by chemical synthesis. However, chemical approaches are based on the use of potentially hazardous substances. Thus, more research is concentrated on alternative production methods. One of them is the synthesis with the use of plant extracts. Biomolecules present in those extracts usually act as both reducing and capping agents. Many of extracts' components have shown to be active against animal and plant pathogens on their own. Depending on the extract used for nanostructure synthesis and experimental conditions, different antimicrobial activity of the final product can be obtained. Because of the multiplicity of factors which may influence on AgNPs activity, the researchers are still investigating new and more efficient ways of AgNPs synthesis.

Since the 12th century carnivorous plants have been used for the treatment of illnesses such as dry cough, bronchitis, whooping-cough, asthma, urinal tract infections or even headache. This is due to their secondary metabolite composition that comprises of flavonoids, naphthoquinones, anthocyanins, phenolic compounds, and organic acids (Juniper et al., 1989). Carnivorous plants belong to a group of endangered species however they can be obtained with a high yield through vegetative reproduction in *in vitro* cultures. This technique allows to increase the propagation rate of valuable, genetically identical plants from even a single plant. Carnivorous plants were used in the pre-antibiotic era and now can return in a modern form to combat antibiotic resistant pathogens (Krychowiak et al., 2014). According to the WHO report on antimicrobial resistance, we may face a post-antibiotic era when even the smallest bacterial infection may become lethal. This urges scientists to search for new ways to cope with this problem.

While searching for new ways of fighting pathogens, sustainability and scalability of the proposed solution must be considered. The twelve principles of green chemistry (Anastas and Warner, 1998) should be taken into account when designing this type of process. This is not only due to the ecological point of view but also economical one. Designing processes for substrate and energy efficiency is a challenging problem in macroscale production. That is why strong emphasis should be placed on those aspects from the beginning of the reaction design. This is especially apparent when considering the heating of the reaction vessel. This is one of the most energy-consuming technological processes that strongly contributes to the profitability of the reaction. Lowering the energy consumption can be beneficial concerning both in the ecological and economical aspects. Bearing in mind silver ion toxicity and biological variability of plant extracts, it is prudent to use an additional capping agent to facilitate the reaction process without the need for full extract standardisation.

To the best of our knowledge, this is the first report describing an easy and eco-friendly biosynthesis method of AgNPs using carnivorous plant extracts. In addition, an antimicrobial potential of obtained AgNPs on both human and plant pathogens had been compared.

2. Materials and methods

2.1. Materials

Silver nitrate was purchased from Merck Millipore. Polyvinylpyrrolidone 4000 (PVP), standards of plumbagin, myricetin, quercetin, hyperoside, ellagic acid, isorhamnetin, were purchased from Sigma Aldrich. Ramentaceone was obtained from the University of Pretoria, Republic of South Africa. Droserone was synthesized by dr E. Paluszkiewicz from the Technical University of Gdansk, according to the method described by Razzakova et al. (1973) and Behrman et al. (1995) with several modifications. Plants: *Drosera indica, Drosera binata, Drosera spatulata,* and *Dionaea muscipula* were grown on solid (0.75% agar), half strength Murashige and Skoog (ø MS) medium (Murashige and Skoog, 1962) with 2% of sucrose and 0.15% activated charcoal at 20 °C, light 30–35 $\mu mol/m^2 \times s$, photoperiod 16/8h, pH 5.5 (Fig. 1). During the whole experiment deionized water was used.

2.2. Preparation of plant extract

Five grams of fresh plant tissue were placed in a 250 mL borosilicate flask. Then 100 mL of water was added. The flask was microwaved for 2 min (Sharp microwave model R-242 (IN)E, 800 W) with a 30-s break after the first minute. After the extract had cooled to room temperature, it was filtered through Whatman No. 1 filter paper. Prior to use, the extract was filtered through 0.22 µm mixed cellulose ester syringe filter to remove residual impurities.

2.3. Preparation of AgNPs – Water bath

Firstly, 400 mg of PVP was added to a 250 mL borosilicate flask. Then 10 mL of plant extract and 90 ml of water was added and everything was thoroughly mixed until complete dissolution of PVP. Subsequently, 100 mL of 8 mM $AgNO_3$ was added to obtain the final 4 mM silver nitrate

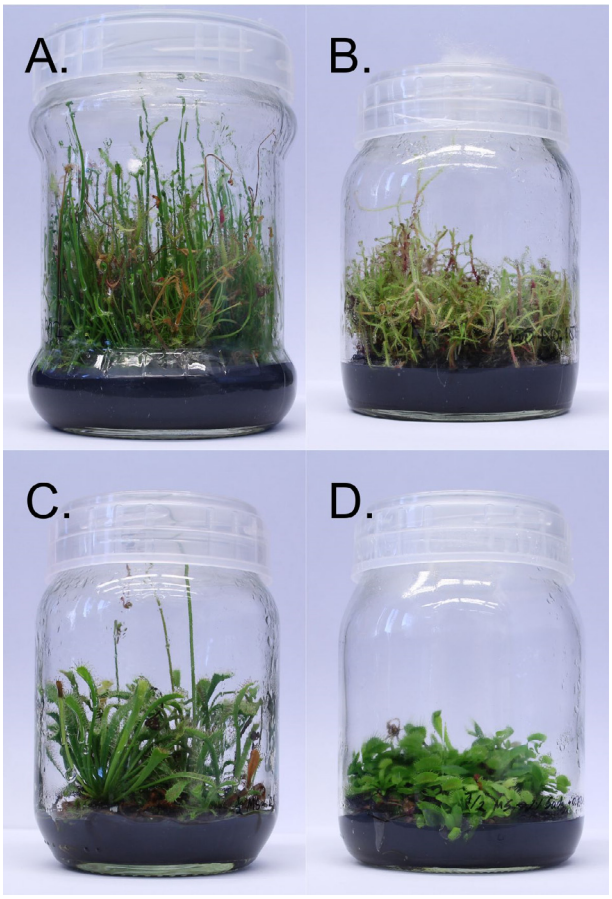

Fig. 1 Growth of carnivorous plants on ø MS medium + 2% sucrose + 0.15% activated charcoal: **A.** *Drosera binata,* **B.** *Drosera indica,* **C.** *Drosera spatulata,* **D.** *Dionaea muscipula.*

concentration. Flasks were incubated in a water bath for 2 h at 70 °C. After the nanoparticle solution had cooled down to room temperature, it was centrifuged for 15 min at 15,000 RCF. The obtained nanoparticle pellet was resuspended in 4 mL of water. The sample was stored at room temperature in darkness for the duration of the tests.

2.4. Preparation of AgNPs – Microwave

Firstly, 200 mg of PVP was added to a 250 mL borosilicate flask. Then, 5 mL of plant extract and 45 mL of water was added and everything was thoroughly mixed until complete dissolution of PVP. Subsequently, 50 mL of 8 mM $AgNO_3$ was added to obtain the final 4 mM silver nitrate concentration. Flasks were microwaved for 2 min with a 30-s break after the first minute. After the nanoparticle solution had cooled down to room temperature it was centrifuged for 15 min at 15,000 RCF. The obtained nanoparticle pellet was resuspended in 4 mL of water. The sample was stored at room temperature in darkness for the duration of the tests.

For the determination of power consumption, GreenBlue GB202 Energy Meter was used each time a synthesis was performed. For the microwave synthesis, the whole energy usage was registered for the sample. For the water bath synthesis, the energy usage was divided between the samples in the water bath. The energy used was measured in Watt-hours.

2.5. Characterization of nanoparticles

AgNPs synthesized with the use of carnivorous plants extracts were characterized by using transmission electron microscopy (TEM), scanning electron microscopy (SEM), dynamic light scattering (DLS), Fourier transform infrared spectroscopy (FT-IR), and X-ray photoelectron spectroscopy (XPS). For TEM analysis samples were placed on grids (Sigma-Aldrich, St Louis, MO, USA) coated with a 2% collodion solution (Sigma-Aldrich). Samples absorbed to the surface were examined using a Philips CM100 electron microscope at 80 kV (FEI Company, Eindhoven, the Netherlands).

The nanoparticles morphology was investigated using scanning electron microscopy (Nova Nano SEM 200, FEI). The observations have been performed taking into account the chemical analysis of specimens in microareas with energy dispersive X-ray spectroscopy (EDS, EDAX). The observations were carried out in low vacuum conditions in the secondary electron mode, using Helix detector. Results are presented in the form of spectra and tables demonstrating the qualitative and quantitative chemical composition of elements occurring in the specimens. The EDS analysis confirmed chemical composition of examined silver nanoparticles.

The particle size distribution in the samples was assessed by dynamic light scattering (DLS) analysis using a Zetasizer Nano ZS (Malvern Instruments Ltd., UK).

The UV–Vis spectra of all samples were recorded with the use of Evolution 300 double beam spectrophotometer equipped with the thermostatic cells. The 200–800 nm range for the measurements was used. All spectra were registered at room temperature. The optical path for all experiments was 1 cm. Spectra were registered for both types of synthesis at intervals ranging from 15 min to 24 h.

Infrared spectra (FT-IR) of AgNPs and carnivorous plant extracts were recorded with the use of potassium bromide (KBr) pellets and Brüker Infrared Spectrometer in the range of 399–4599 cm^{-1}. AgNPs samples, as well as extracts, were lyophilised before the forming of KBr pellets.

X-ray Photoelectron Spectroscopy analysis (XPS) was carried out with the use of X-ray photoelectron spectrometer (Omicron NanoTechnology) with a 128-channel collector. XPS measurement has been done at room temperature in ultra-high vacuum conditions below 1.1×10^{-8} mBar. The photoelectrons were excited by a Mg-Kα X-ray source. The X-ray anode was operated at 15 keV and 300 W. Omicron Argus hemispherical electron analyser with round aperture of 4 mm was used for analysis of emitted photoelectrons. The binding energies were corrected using the background C1s line (285.0 eV) as a reference. XPS spectra were analysed with Casa-XPS software using a Shirley background subtraction and Gaussian–Lorentzian curve as a fitting algorithm.

2.6. HPLC analysis

The chromatographic separation was carried out using Beckmann Gold System equipped with a Thermo Separations Spectra 100 variable wavelength detector and a Rheodyne 6-way injection valve. For the stationary phase, an Agilent Zorbax SB-Phenyl (4.6 × 150 mm, 3.5 µm) was used. The flow rate used was 1 mL min^{-1}. The sample injection volume was 10 µL. The mobile phase for the analysis consisted of 0.1%

(v/v) trifluoroacetic acid in acetonitrile as eluent A; 0.1% (v/v) trifluoroacetic acid in water as eluent B. The separation gradient was 0 min (10% A)-> 5 min (10% A)-> 12 min (90% A)-> 20 min (90% A) followed by a 10-min column regeneration. Chromatographic separations were carried out at room temperature. Typical compounds present in carnivorous plant tissues (droserone, hyperoside, ellagic acid, myricetin, ramentaceone, plumbagin, quercetin, isorhamnetin) were used as standards to determine the extracts composition. Three level standard curve was used for determining the concentration of the compounds 4-point. Monitoring was performed at 254 nm. All analyses were performed in triplicate.

2.7. DPPH radical scavenging assay

The antioxidative properties of water extracts from *Drosera* and *Dionaea* species were evaluated with the use of the DPPH (2,2-diphenyl-1-picrylhydrazyl free radical) assay, which measures the ability of chemicals to reduce DPPH radical. Free radical scavenging activity of extracts used in silver nanoparticles synthesis was determined according to the method described by Abdelwahab et al. (2014) with minor modifications. The final concentration of DPPH radical in the assay was 0.1 mM. Working solutions of extracts and DPPH radical were prepared in pure methanol. Each extract was tested at the concentration ranging from 1.25 to 25 mg of fresh weight (FW) mL^{-1}. Conversion of 2,2-diphenyl-1-picrylhydrazyl free radical into diphenyl-1-picrylhydrazyl (DPPH) was measured spectrophotometrically at 517 nm (EnVision Multilabel Reader, Perkin Elmer) after 30 min incubation at room temperature in the dark. The inhibition of DPPH radical absorbance was calculated according to the formula:

$$\text{Inhibition } (\%) = \text{Abs}_{(C)} + \text{Abs}_{(S)}/\text{Abs}_{(C)} \times 100, \quad (1)$$

where $\text{Abs}_{(C)}$ is the absorbance of control (DPPH radical) and $\text{Abs}_{(S)}$ is the absorbance of extract sample. All analyses were performed in triplicate.

2.8. Study of antimicrobial and antifungal susceptibility

The antimicrobial and antifungal activity of AgNPs were determined using the Broth Microdilutions Method according to guidelines provided by the Clinical and Laboratory Standards Institute. To determine minimal inhibitory concentration (MIC), minimal bactericidal concentration (MBC) and minimal fungicidal concentration (MFC) of AgNPs, tests on 96-well plates were performed. Two species of human bacterial pathogens: G (+) *Staphylococcus aureus* Newman (Duthie and Lorenz, 1952) and G (−) *Pseudomonas aeruginosa* PAK (Ramphal et al., 2008), fungi *Candida albicans* ATCC 90028, and three G (−) plant pathogens: *Pectobacterium atrosepticum* SCRI 1043, *Pectobacterium parmentieri* Scc3193 (earlier *Pectobacterium wasabie*) and *Dickeya dadantii* 3937, were used throughout our study. All human pathogens were grown overnight in Brain Heart Infusion (BHI) medium (BTL, Poland) at 37 °C, plant pathogens on Lysogeny Broth (LB) medium (Roth, Germany) at 28 °C (*Pectobacterium*) and at 37 °C (*Dickeya*). All tested microorganisms are deposited at the IFB, UG & MUG, Poland. Overnight bacterial cultures were diluted to obtain the initial inocula, equivalent to 0.5 McFarland turbidity standard measured by densimeter (DensiMeter II, EMO, Brno). AgNPs from carnivorous plants (in a range of 1–100 µl mL^{-1} which correspond to 1.7–170 µg nanoparticles/mL) were applied into wells of the 96-well plate and suspended in BHI or LB medium (final volume of the medium was 100 µL). Water extracts (after evaporation) from four species of carnivorous plants were also tested in a range of 1–1000 µl mL^{-1}. The suspension of 0.5 in McFarland scale of bacteria or fungi was diluted (final 1.5×10^5 CFU/mL for bacteria and 1.5×10^4 CFU/mL for fungi) in LB or BHI medium, and 10 µL was added into wells. The plates were incubated at 28 °C or 37 °C for 24 h and the MIC was established. Then, 100 µL of the suspension was plated onto Luria Agar (LA) or BHI Agar medium. Plates were incubated at 28 °C or 37 °C for 24 h and at room temperature for 24 h and the MBC was established. All analyses were performed in triplicate. The *in vitro* activity of antibiotics: vancomycin – glycopeptide (Sigma-Aldrich), ciprofloxacin – second-generation fluoroquinolone (Sigma-Aldrich), oxacillin – penicillinase-resistant β-lactam (Sigma-Aldrich), cefotaxime – cephalosporin III generation (Ranbaxy, India), piperacillin – β-lactam (Sigma-Aldrich), ceftazidime third-generation cephalosporin (Sigma-Aldrich) and streptomycin – aminoglycoside (Sigma-Aldrich) against bacteria, and fluconazole (Sigma-Aldrich) and amphotericin (Sigma-Aldrich) against fungi was evaluated for comparison purposes. We also tested commercially available silver nanoparticles AgNPs (NanoAmor company, USA) with a purity of 99.9%, 80 nm particle size and density of 10.49 g/cm^3 (catalog number 7440-22-4), and AgNPs_COOH (provided by ProChimia Surfaces Co. (Poland) as water-soluble nanoparticles coated with the HS-(CH2)10-$COOH^+$ ligand, 5.5 nm in diameter, characterized by a dispersity level of 15%. The initial stock concentration of AgNPs was 10.5×10^{14} NPs mL^{-1} which corresponds to 958 µg mL^{-1} (SPR maximum, λ_{max}: 420–424 nm).

3. Results

3.1. Preparation and characterization of AgNPs in water bath or with the use of microwaves and its characterization

After incubation in the water bath the solutions' colours turned from dark yellow to deep red that is consistent with nanoparticle colloid solutions. In low lighting conditions, the colloid seemed to be clouded. Straight after microwave-assisted synthesis solutions showed a much lighter colour than their counterparts synthesized in the water bath. After cooling down to room temperature the difference in colouration was insignificant.

Transmission and scanning electron microscopy images showed the differences in the morphology of AgNPs (Fig. 2). Depending on the type of extract different size of the nanoparticles were observed. Nanoparticles synthesized using *D. muscipula* (Fig. 2: A4, B4, A8, B8) and *D. indica* (Fig. 2: A2, B2, A6, B6) extracts showed high concentration and shape uniformity. We did not observe homogeneity in shape for AgNPs from *D. binata*. The SEM images revealed the formation of even 300 nm clusters. The sizes of the most antimicrobial active *D. indica* and *D. muscipula* nanoparticles are presented in Fig. 3. The water bath synthesized samples showed a considerable fraction of small (~5–10 nm) nanoparticles (Fig. 2: A1, B1, A2, B2, C1, C2, D1, D2).

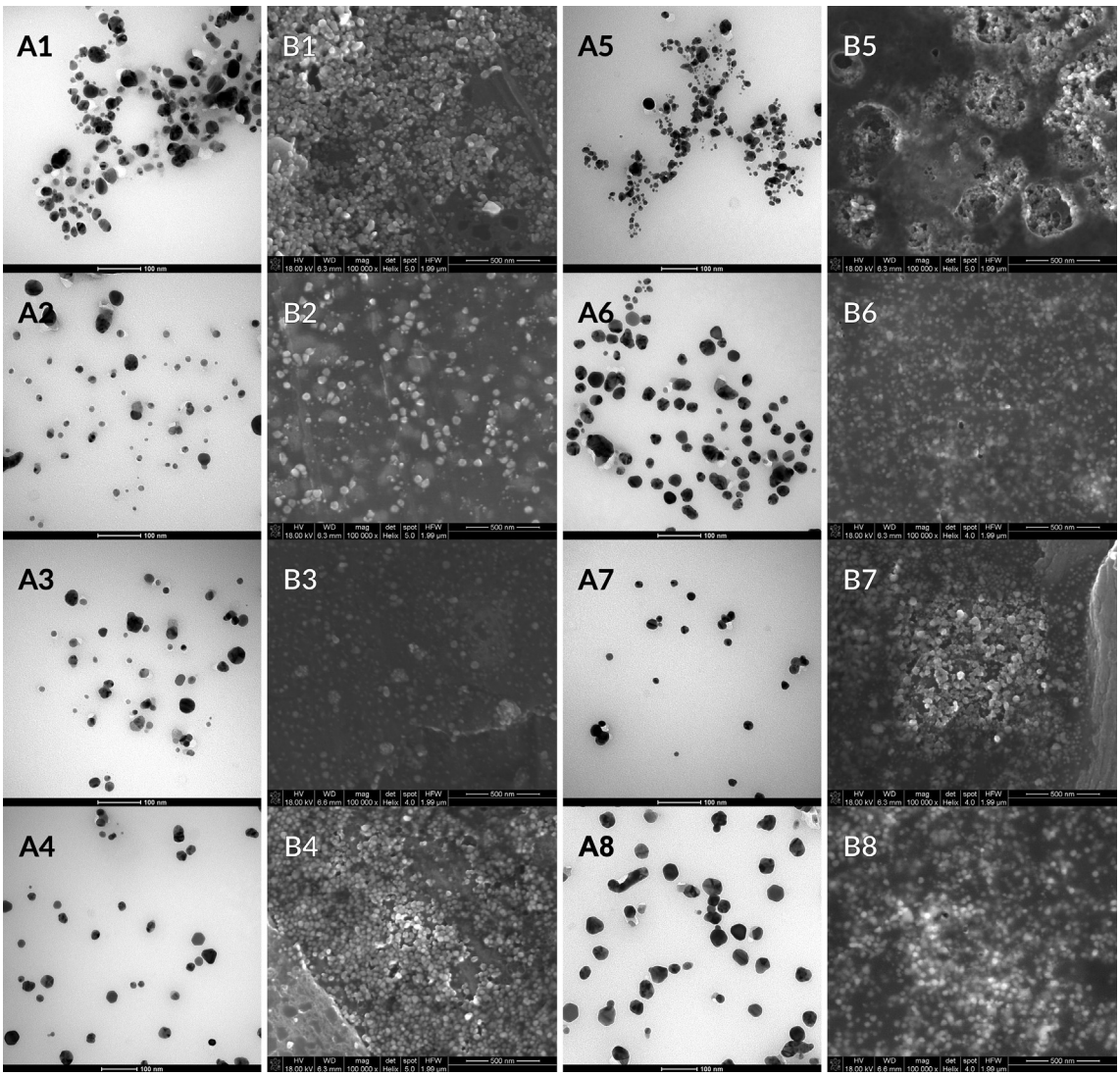

Fig. 2 TEM (A) and SEM (B) images of silver nanoparticles synthesized using: 1, 5 – extracts from *D. binata*, 2, 6 – extracts from *D. indica*, 3, 7 – extract from *D. spatulata*, 4, 8 – extract from *D. muscipula*. 1–4 AgNPs obtained in water bath, 5–8 AgNPs obtained in microwave.

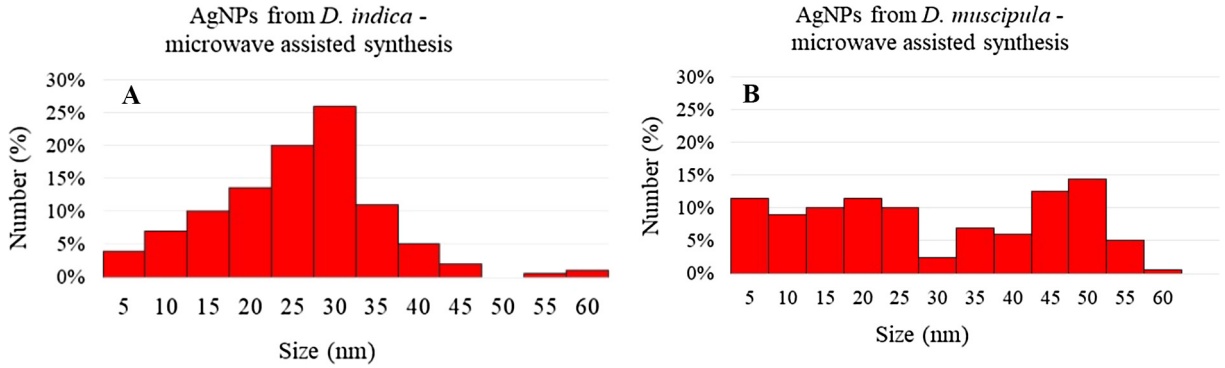

Fig. 3 The particle size distribution of the samples (A) AgNPs from *D. indica* using microwave assisted synthesis, (B) AgNPs from *D. muscipula* using microwave assisted synthesis assessed by dynamic light scattering.

Fig. 4 shows an example of EDS analysis of AgNPs obtained from *D. muscipula*. The EDS spectrum mainly consists of C, O and Ag peaks. The high content of carbon element corresponds to carbon tape, which was used for nanoparticles mounting. The oxygen concentration in amount of 11% is related to the aqueous solution. The EDS analysis and electron

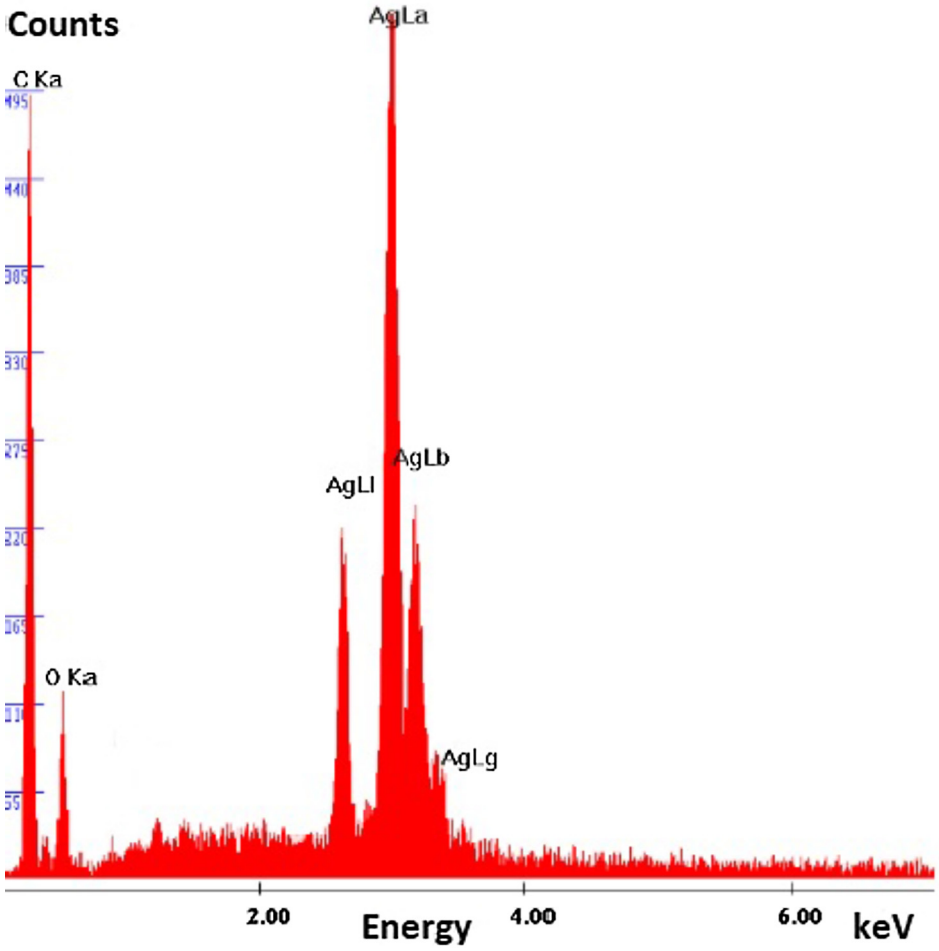

Fig. 4 EDS spectrum for the AgNPs synthesized using microwave assisted synthesis of water extract from *D. muscipula*. The spectrum consisted of different peaks for silver (Ag), carbon (C), and oxygen.

diffraction pattern suggest that the nanoparticles are only composed of Ag element. Similar results were obtained for the other AgNPs (data not shown).

The UV–Vis spectra of the silver nanoparticles (AgPNs) formation process with the use of water bath and microwave are presented in Fig. 5 and Fig. 6, respectively. Colour of nanoparticle solutions change from light-yellow to dark-brown through the reaction. The UV–Vis spectra were recorded at different time intervals (15 min, 1 h, 3 h, 6 h, 9 h, 12 h and 24 h) to observe the gradual reduction of silver nitrate in solution after treatment with microwaves of high temperature. The UV–Vis spectra of each AgNPs species recorded after 24 h showed that the absorbance maximum did not change significantly in respect to the 12 h spectrum. The results confirmed that the reaction reached its equilibrium within 24 h. The final spectra for each type of AgNPs showed a characteristic peak at c.a. 420 nm. This peak corresponds to silver nanoparticles appearance in solution and it was present in all tested mixtures. Furthermore, the comparison of UV–Vis spectra (Fig. 7) of carnivorous plant extracts and AgNPs spectra proves that both methods can be used to obtain silver nanoparticles. Additional information about UV–Vis spectral characteristics of other substances used during both synthesis pathways (aqueous solutions of silver nitrate, PVP, plant extracts and PVP/extract solutions) can be found in Supplementary Information, see Fig. S1.

FT-IR spectra of AgNPs together with spectra of plant extracts used for the synthesis are shown in Fig. 8. It is worth mentioning that the FT-IR spectra of AgNPs obtained by using two independent methods are similar, although the spectra for the microwave method are more explicit aiding in the AgNPs derivatisation identification. FT-IR analysis showed that after AgNPs formation, their binding with compounds from the plant extract is possible and is due to the interactions between the —OH and the C═O groups of appropriate polyphenolic compounds in plant extracts. IR spectra carnivorous plant/AgNPs systems illustrate the mentioned phenomenon, with the regions of relevance shown in Fig. 8. The high intensity peaks at 557 and 636 cm^{-1} indicate the presence of uncoated AgNPs in case of all studied samples. Additionally, there are significant shifts in the —OH and C═O peaks, while all the other peaks (mainly aliphatic and aromatic C—H stretching) remain unchanged. The shifts observed for stretch —OH and C═O were following: 166 and 87 cm^{-1} (*D. binata* extract); 134 and 71 cm^{-1} (for *D. indica* extract); 158 and 71 cm^{-1} (*D. spatulata* extract); 110 and 63 cm^{-1} (*D. muscipula* extract), respectively. These spectral changes may be related to AgNPs coating by compounds from

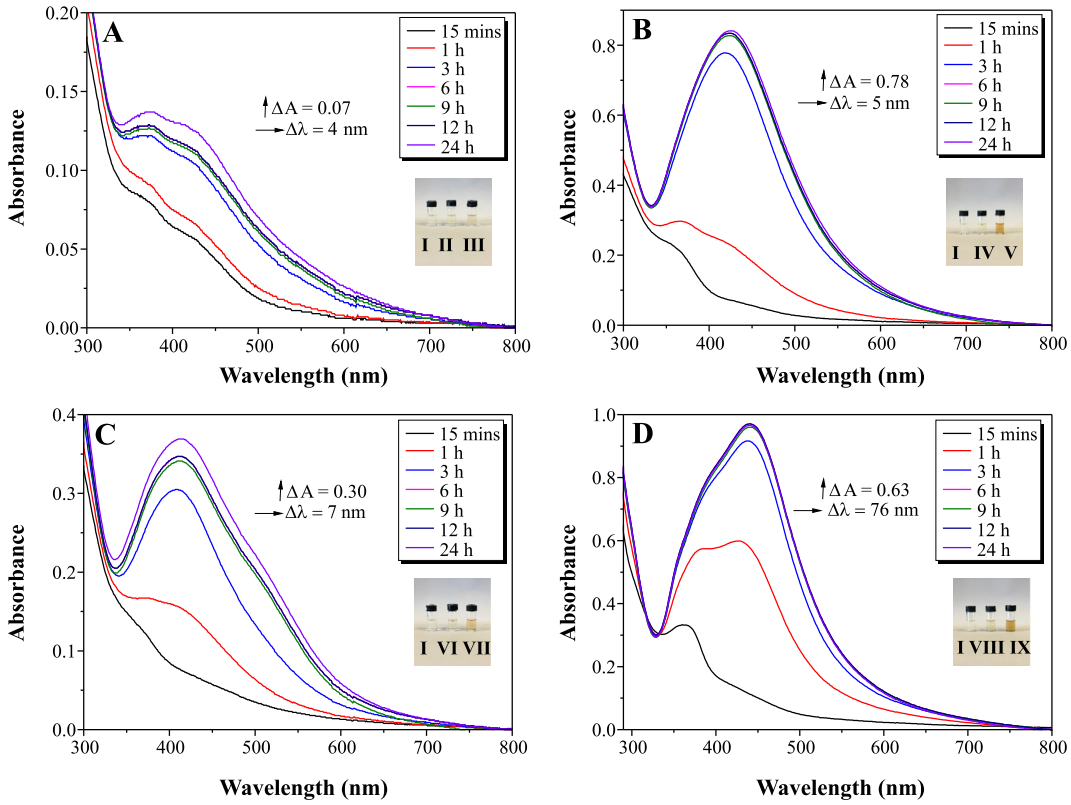

Fig. 5 Time dependent UV–Vis spectra confirming the AgNPs formation by using water bath method in the presence of: (A) *D. binata*; (B) *D. indica*; (C) *D. spatulata*; (D) *D. muscipula*; **I-IX** aqueous solutions of: **I** – $AgNO_3$; **II**, **IV**, **VI**, **VIII** – pure, appropriate plant extracts of *Drosera*; **III**, **V**, **VII**, **IX** – adequate *Drosera*/AgPNs systems obtained.

carnivorous plant extracts in studied solutions. Additional information about FT-IR spectral characteristics of other substances used during both synthesis methods (silver nitrate, PVP, plant extracts and PVP/carnivorous plant combinations) can be found in Supplementary Information, Fig. S2.

XPS experiment has been performed to provide insight on valance state of silver nanoparticles in sample obtained from *D. muscipula* extract using microwave-assisted synthesis method. Exemplary spectra of such samples are presented in Fig. 7. $Ag3d_{5/2}$ and $Ag3d_{3/2}$ photoelectron peaks of silver have been observed at 368.22 and 374.21 eV respectively. Spin orbit components in all cases were separated by distance of 6 eV which is characteristic for silver. Shape of obtained spectra is comparable to the ones published before (Prieto et al., 2012). However, it is difficult to distinguish between different silver state components of $3d_{5/2}$ peak. Therefore, definition of silver oxidation state on the basis of XPS measurements is challenging and sometimes impossible. Consequently, modified Auger parameter (α') had to be calculated. In order to acquire it, kinetic energy of silver M4VV Auger line was determined (presented in Fig. 9) at position equaled 357.1 eV. Parameter has been calculated according to the equation:

$$\alpha' = BE(Ag3d_{5/2}) + KE(AgM4VV) \quad (2)$$

where BE($Ag3d_{5/2}$) is the binding energy of $Ag3d_{5/2}$ peak and KE(Ag M4VV) is kinetic energy of M4VV Auger line peak. Parameter α' for metallic silver equals 726 eV (Ramstedt and Franklyn, 2010). Calculated result for our sample is 725.3 eV, which means that most of Ag oxidation states existed in Ag^0 form. Similar results were obtained for the other AgNPs (data not shown).

3.2. HPLC analysis

HPLC analysis revealed that main compounds in the water extracts belong to the flavonoids and naphthoquinones groups (Table 1, Fig. 10). The concentration of those compounds differed between carnivorous plant species. From all tested plants *D. muscipula* tissue was most abundant in secondary metabolites. From the three species of *Drosera*, the most abundant with secondary metabolites were *D. indica* extracts. Each of the samples had relatively high concentration of hyperoside and ellagic acid (Fig. 10). The highest concentration of ellagic acid and hyperoside was found in *D. musciplula* and *D. indica* respectively. Depending on the tissue, plumbagin (in *D. muscipula* and *D. binata*), ramentaceone (in *D. spatulata*) or plumbagin and ramentaceone (in *D. indica*) was found. The total concentration of naphthoquinones was similar among tested samples except *D. spatulata* extract in which the concentration of ramentaceone was 16.397 μg mL^{-1}. Myricetin and isorhamnetin in larger concentrations were only found in *D. muscipula* tissues (Table 1, Fig. 10).

3.3. DPPH radical scavenging assay and study of antimicrobial susceptibility

Plant extracts obtained after the microwave-assisted extraction showed light to dark yellow colour shift. This was due to the

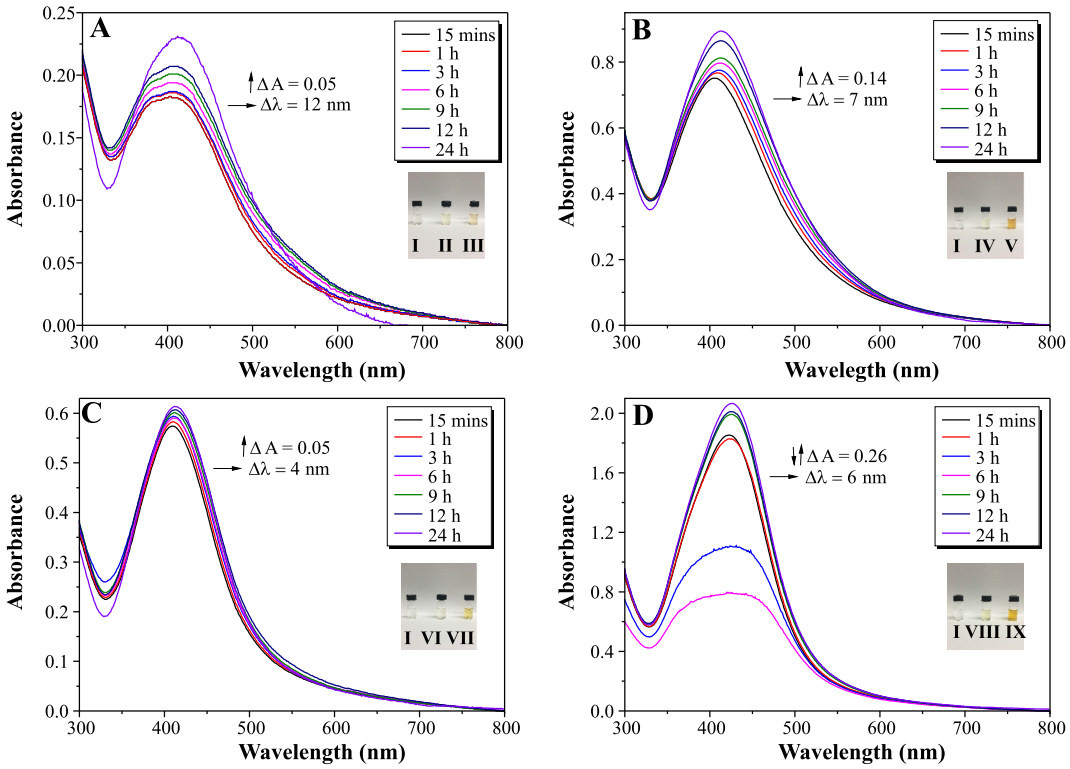

Fig. 6 Time dependent UV–Vis spectra confirming the AgNPs formation by using microwave method in the presence of: (A) *D. binata*; (B) *D. indica*; (C) *D. spatulata*; (D) *D. muscipula*; **I-IX** aqueous solutions of: **I** – $AgNO_3$; **II**, **IV**, **VI**, **VIII** – pure, appropriate plant extracts of *Drosera*; **III**, **V**, **VII**, **IX** – adequate *Drosera*/AgPNs systems obtained.

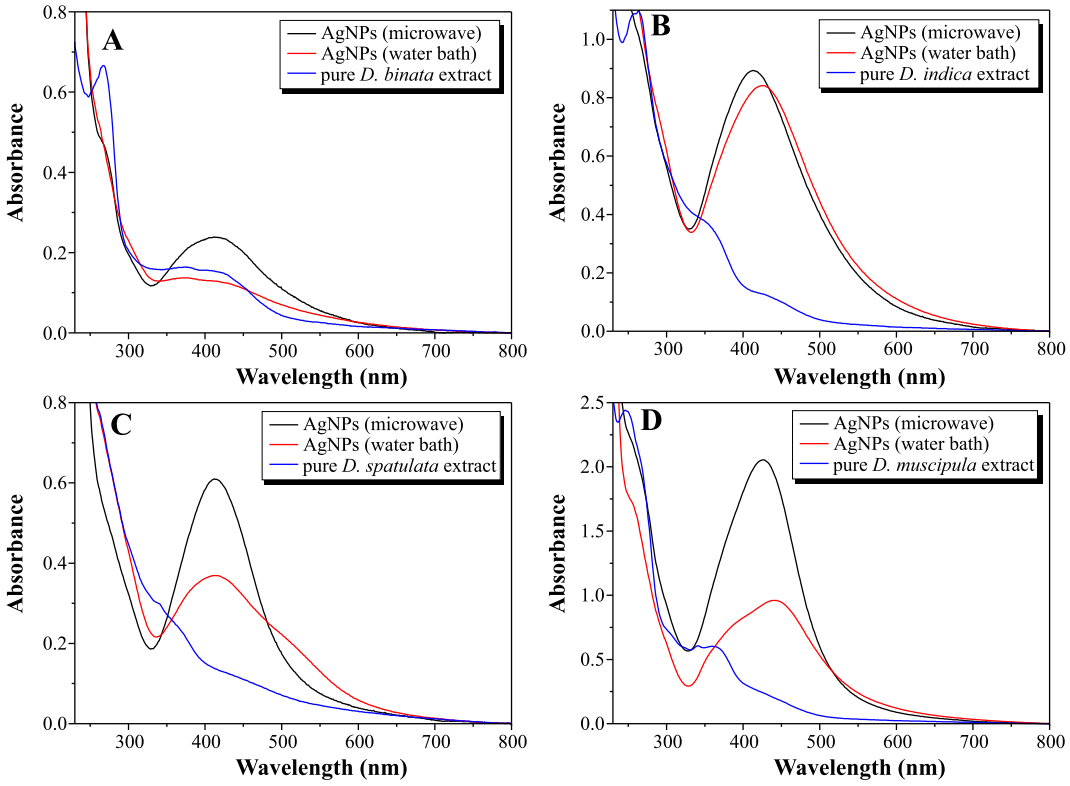

Fig. 7 The spectral comparison of appropriate substrates (pure aqueous *Drosera* extracts) with products obtained (AgNPs) by microwave and water bath assisted synthesis: (A) *D. binata*; (B) *D. indica*; (C) *D. spatulata*; (D) *D. muscipula*.

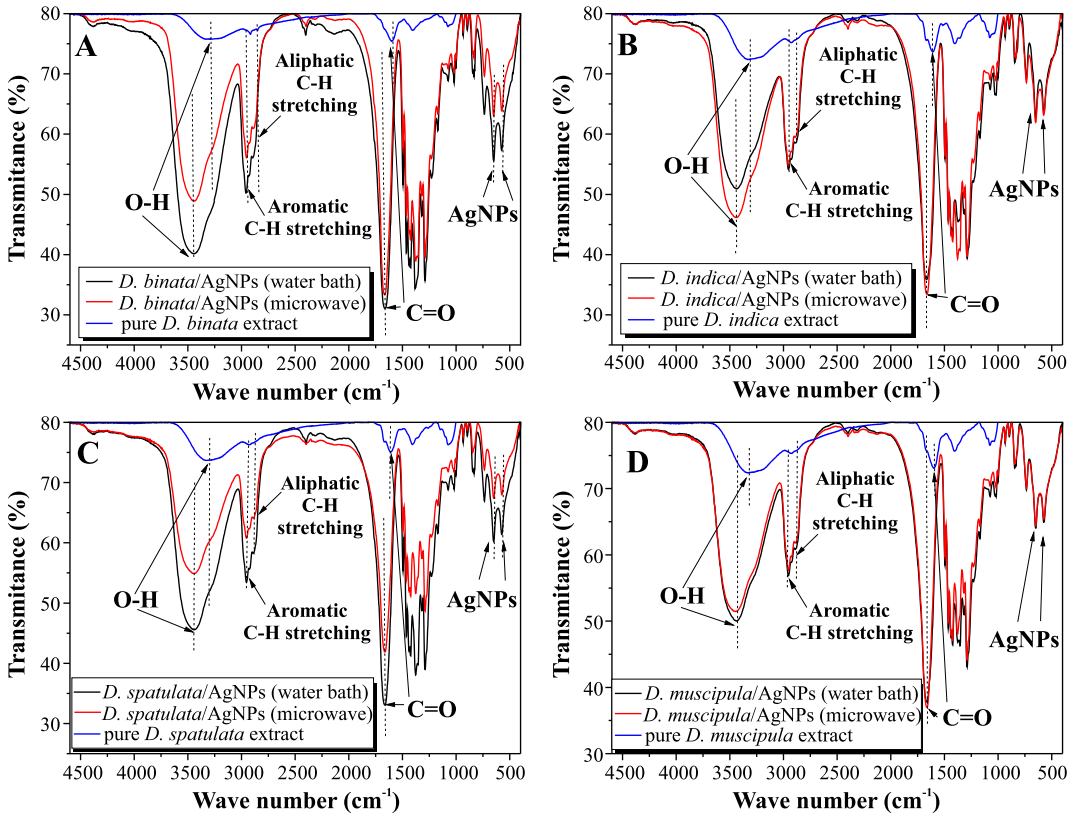

Fig. 8 The FT-IR spectra of *Drosera*/AgNPs systems obtained by using two independent synthetic methods with additional Fourier transform infrared spectra of appropriate plant extracts: (A) *D. binata*; (B) *D. indica*; (C) *D. spatulata*; (D) *D. muscipula*.

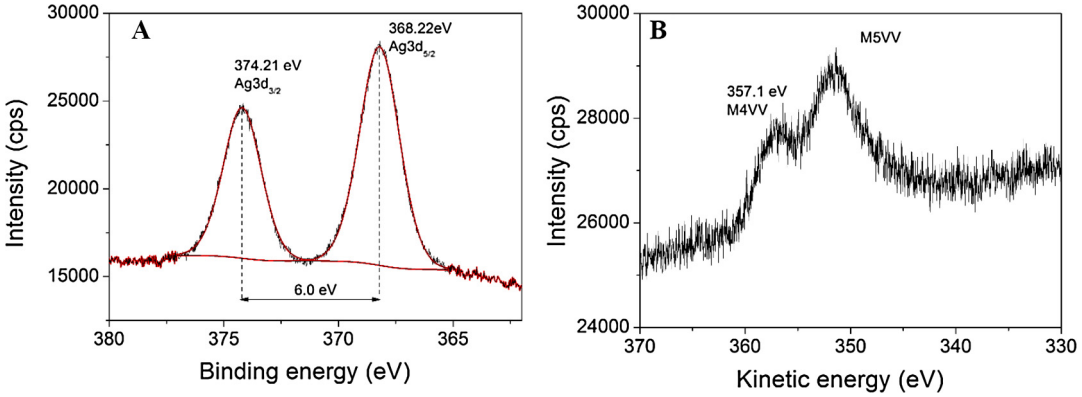

Fig. 9 XPS spectra for Ag 3d region (A) and Auger lines (B) of AgNPs synthesized using microwave assisted synthesis of water extract from *D. muscipula* sample.

solubilization of flavonoids and other water-soluble compounds present in the plant tissue. In order to evaluate the antioxidative activity of water extracts of *D. muscipula*, *D. binata, D. indica* and *D. spatulata*, their ability to scavenge DPPH free radicals was analysed. Both *D. muscipula* and *D. indica* possessed similar and the highest radical scavenging properties (IC_{50} = 0.857 ± 0.023 mg FW mL^{-1}) despite their various secondary metabolite composition (Table 1). DPPH test revealed that *D. binata* extract possessed the lowest radical scavenging potential out of the four tested extracts, because the IC_{50} was 5.5 ± 0.049 mg FW mL^{-1}. The IC_{50} of the water extract for *D. spatulata* was 1.428 mg ± 0.029 FW mL^{-1}. It is worth mentioning that radical scavenging properties of plants extracts were strongly correlated with the antimicrobial activity of AgNPs obtained using the aforementioned plant extracts.

Synthesized nanoparticles showed higher antimicrobial activity against plant pathogens in comparison to human pathogens (Table 2). The Minimal Inhibitory Concentration varied depending on the microorganism and was between 5.3 µg mL^{-1} (for *D. dadantii* and *P. aeruginosa*) and 170 µg mL^{-1} or more (for *S. aureus* and *C. albicans*). The highest

Table 1 Chromatographic data of compounds identified by HPLC in the water extract from four extracts from carnivorous plants.

Compound	Concentration [μg mL^{-1}]			
	Drosera binata	*Drosera indica*	*Drosera spatulata*	*Dionaea muscipula*
Hyperoside	15.290 ± 0.362	44.813 ± 0.237	15.136 ± 0.205	12.207 ± 0.286
Elagic acid	14.968 ± 0.273	36.751 ± 0.496	36.198 ± 0.307	104.303 ± 0.510
Myricetin	0.107 ± 0.002	6.062 ± 0.175	3.320 ± 0.080	59.241 ± 2.312
Quercetin	0.511 ± 0.009	2.236 ± 0.076	0.893 ± 0.012	3.945 ± 0.112
Isorhamnetin	0.403 ± 0.027	0.683 ± 0.059	0.375 ± 0.044	1.592 ± 0.024
Droserone	1.012 ± 0.022	1.631 ± 0.055	2.162 ± 0.013	3.314 ± 0.051
Plumbagin and ramentaceone	45.681 ± 0.145	52.647 ± 0.356	16.397 ± 0.789	53.147 ± 0.583

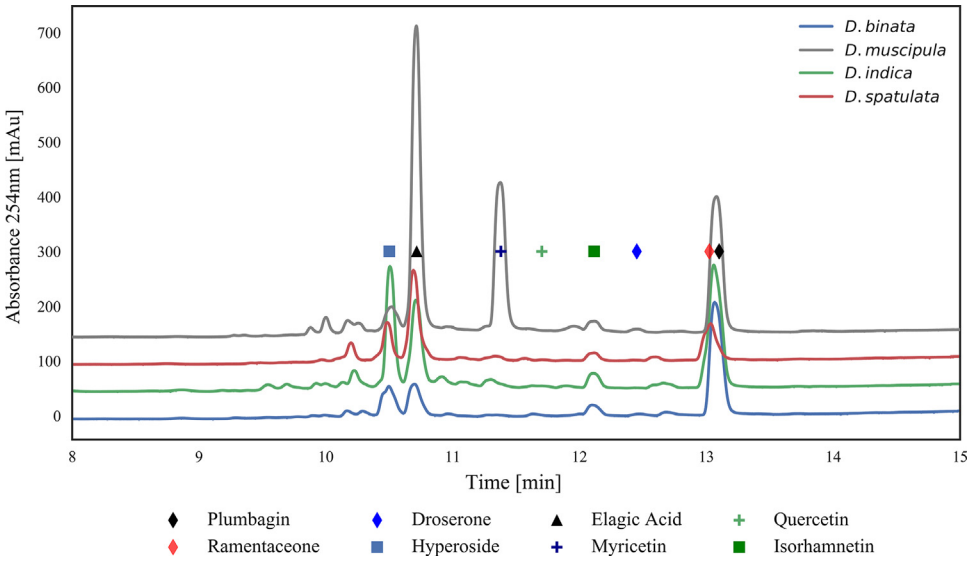

Fig. 10 HPLC analysis of water extracts from *D. binata, D. muscipula, D. indica* and *D. spatulata*.

antimicrobial activity for both pathogens was shown by AgNPs synthesized using the microwave method and extracts from *D. muscipula* and *D. indica* because the range of MBC was between 5.3 μg mL^{-1} and 42.5 μg mL^{-1} (Table 2). The most resistant to AgNPs was fungi (*C. albicans*) where MBC was above 170 μg mL^{-1}. Water extracts from carnivorous plants tested in the range from 1 to 1000 μl mL^{-1} did not show antimicrobial activity against tested microorganisms (data not shown).

4. Discussion

Green synthesis is energy efficient, easy and fast. It allows avoiding the use of toxic and dangerous compounds, so it does not harm the environment (Mohapatra et al., 2015; Zhang et al., 2016). In this method, different biological systems, including bacteria, fungi and plants, are used for the production of nanoparticles (Liu et al., 2012; Zhang et al., 2016). Biological synthesis methods allow controlling the size and shape of nanoparticles. These are important factors considering their biomedical use (Gurunathan et al., 2009). AgNPs have already been synthesized using plant extracts from: *Magnolia grandiflora* and *Eucalyptus angophoroides* (Okafor et al. 2013), *Citrus limon* (Prathna et al., 2011), *Capsicum annuum* L. (Li et al., 2007), *Camellia sinensis* (Loo et al., 2012), *Cinnamomum altissimum* Kosterm. (Abdelwahab et al., 2017), coffee and green tea (Rónavári et al., 2017), olive leaves (Khalil et al., 2014), and many others. In our research, we used biomolecules from carnivorous plants' extracts as a reducing and capping agent for the green synthesis of nanoparticles characterized by high antimicrobial activity.

Drosera and *Dionaea* tissues are a natural source of pharmacologically important compounds (e.g. glucosides, flavonoids, phenolic acids) that are used as substrates in the production of pharmaceuticals (Kreher et al., 1990, Finnie and van Staden, 1993). Our previous studies have shown that chloroform and methanol extracts from *Drosera* sp. and *Dionaea* tissues have a great antimicrobial potential (Krolicka et al., 2008, 2009, 2010; Szpitter et al., 2014; Taraszkiewicz et al., 2012). This study answers the question whether secondary metabolites from carnivorous plants are a good basis for AgNPs synthesis and whether the resulting AgNPs would possess higher antimicrobial activity than the extracts that were used for their preparation.

4.1. Preparation of AgNPs – Water bath and microwaves-assisted

Already published studies showed that the synthesis of most AgNPs with the use of plant extracts do not require an addi-

Table 2 Comparison of Minimum Bactericidal/Fungicidal Concentrations (MBCs/MFCs) of AgNPs synthesizes by using different carnivorous plant tissue, commercially available AgNPs and antibiotics.

Human and plant pathogenes	AgNPs – water bath assisted synthesis				AgNPs – microwave assisted synthesis				AgNPs NanoAmor	AgNPs with HS-(CH2)10-COOH$^+$ ligand	Antibiotics
	Drosera binata MBC/MFC* (μg mL^{-1})	*Drosera indica*	*Drosera spatulata*	*Dionaea muscipula*	*Drosera binata*	*Drosera indica*	*Drosera spatulata*	*Dionaea muscipula*			
Staphylococcus aureus Newman	170	170	153	170	127.5	21.2	85	21.2	< 150	13.4	VAN – 32 OXA – 0.25 CIP – 0.5
Pseudomonas aeruginosa PAK	42.5	34	34	34	85	5.3	42.5	5.3	< 150	6.0	PIP – 4.0 CEF – 1.0 CIP – 0.25
Candida albicans ATCC 90028	< 170	< 170	< 170	< 170	170	42.5	85	42.5	< 150	23.9	AMP – 0.25 FLUC – 5.0
Pectobacterium atrosepticum SCRI 1043	21.2	5.3	10.6	5.3	10.6	5.3	5.3	5.3	< 150	0.8	CEF – 1 STR – 32
Pectobacterium parmentieri Scc 3193 (earlier *Pectobacterium wasabie*)	21.2	10.6	21.2	21.2	10.6	10.6	10.6	10.6	< 150	12	CEF – 1 STR – 32
Dickeya dadantii 3937	21.2	10.6	21.2	21.2	21.2	10.6	21.2	7.9	< 150	12	CEF – 1 STR – 64

VAN – Vancomycin; OXA – Oxacillin; CIP – Ciprofloxacin; PIP – Piperacillin; CEF – Ceftazidime; AMP – Amphotericin; FLUC – Fluconazole; CEF – Cefotaxime; STR – Streptomycin.

tional capping agents. While AgNPs were obtained by synthesis based on carnivorous extracts potential and without the use of additional capping agents they occurred unstable and aggregated during the synthesis, forming a grey-silver suspension that precipitated within two hours. Addition of polyvinylpyrrolidone (PVP) as a capping agent in concentration 200 mg 100 mL^{-1} as previously reported (Banasiuk et al., 2016) enabled the formation of stable colloids in both microwave and water bath assisted synthesis. Polyvinylpyrrolidone is usually used as an additive in the microwave assisted polyol AgNPs synthesis methods (Kim et al., 2006). It is also used as a capping agent for microwave assisted synthesis in water environment with pure/synthetic compounds as reducing agents (Nadagouda et al., 2011). Using capping compounds with plant extracts is usually omitted as the components of the extract can act both as reducing and capping agents. During this study, we tested the influence of PVP on the process. PVP acted only as an end-capping/stabilizing agent. In the control reactions without plant extract, synthesis of the nanoparticles was not observed. This additive is essential for AgNPs formation if the extract possesses high reducing and low capping capabilities. After microwave irradiation, the solution colour had gradually changed over time until the solution reached room temperature. This would suggest that the process continues even after heating of the sample is stopped. It has been previously shown (Bilecka and Niederberger, 2010) that the microwave assisted synthesis is an economical way for delivering heat energy to the reaction vessel. Power consumption during the microwave synthesis was 42 ± 1 Wh per sample, whereas during the water bath synthesis it was 65.25 ± 3 Wh. The value presented for the water bath synthesis does not take into account the energy needed to heat the water bath to the required 70 °C. When considering the whole process, the energy consumption was 249 ± 3 Wh per sample. Taking into consideration the time needed for the process, the use of microwave-assisted synthesis gives an economical advantage for small to medium-scale nanoparticle synthesis processes. On the other hand, large-scale and continuous production of nanoparticles may benefit economically from water/oil bath synthesis since the apparatus is inexpensive and commercially available but the process should be thoroughly optimised. This is due to the nature of the heat distribution in the reaction vessel. Heat distribution using microwaves is more efficient and uniform. Apart from shortening the heating time microwave irradiation can suppress side reactions that would hinder the activity of the final product (Bilecka and Niederberger, 2010). To achieve this in a conventional heating method the reaction vessel should have a capillary diameter.

4.2. Characterization of nanoparticles

We observed a correlation between the DPPH scavenging activity of the used extracts, and the size and number of nanoparticles. Nanoparticles synthesized using *D. binata* extract formed larger clusters. This might explain their lower antimicrobial activity. Aggregation process has an impact on the surface to mass ratio of AgNPs and thus reduces antimicrobial activity of nanostructures as their surface, binding to the microbial cells, decreases (Morones et al., 2005; Rai et al., 2012). Smaller nanoparticles are usually more desired since they show higher antimicrobial activity (Pal et al.,

2007) but this fact is inconsistent with our observed results. We found that larger but similar in size nanoparticles show higher antimicrobial activity rather than those with heterogeneous size distribution.

The samples after the reaction change from light to dark brown in colour (Figs. 5 and 6, insert). For all samples the absorbance maximum was registered at about 420 nm. This indicates the presence of silver nanoparticles. The detailed FT-IR analyses confirmed the presence of AgNPs partially coated with PVP and showed the binding mode between AgNPs and plant extracts components.

4.3. Preparation of plant extract and DPPH radical scavenging assay

The results obtained with DPPH radical scavenging assay for water extracts from carnivorous plants clearly correlated with antimicrobial activity. The most potent AgNPs were synthesized in plant extracts with the highest antioxidant potential (Table 2). The flavonoids from *Drosera* sp. and *Dionaea* tissues were crucial in the synthesis of AgNPs. They were responsible for the reduction of silver ions and partially for the stabilization of the obtained nanoparticles. Qin et al. (2010) showed that it is possible to obtain silver nanoparticles by using ascorbic acid (very potent antioxidant) as a reductant. It was shown so far by Krolicka et al. (2009) that the methanol extract (containing flavonoids like quercetin and myricetin) from *Drosera aliciae* proved to be a very potent antioxidant. The highest concentrations of flavonoids in *D. muscipula* and *D. indica* and AgNPs obtained from these tissues were most active against bacteria and fungi. Our research showed that flavonoids from carnivorous plants possess high antioxidant properties and thus are also excellent silver ions bioreductans.

4.4. Study of antimicrobial susceptibility

Bacteria employ various mechanisms to survive in unfavourable environmental conditions. Widespread application of antibiotics caused the emergence of antibiotic-resistant bacterial phenotypes. Therefore, a lot of effort is put into discovering novel classes of antimicrobial compounds, with a mode of action distinct from antibiotics (Singh and Barrett, 2006). Bacterial cell structure is an important factor for the antimicrobial effectivity of compounds. In our research, we have shown that G (−) bacteria, especially plant pathogens, are more susceptible to AgNPs compared to Gram positive bacteria. This is due to the differences in the structure of cell membrane and cell wall between Gram (+) and Gram (−) bacteria (Dakal et al., 2016). Negatively charged bacterial cell membranes and cell wall are the main sites of attachment for positively charged AgNPs. Silver nanostructures aggregate on the bacterial cell surface and therefore disrupt its functions. However, AgNPs are also able to penetrate the bacterial cell membrane and subsequently enter the cytoplasm where highly reactive silver ions are released from their surface. As Ag^+ ions released intracellularly play a crucial role in bactericidal activity, the rate of membrane penetration renders gram negative bacteria more susceptible to silver nanoparticles.

Ansari et al. (2011) have determined the MBC value for commercial nanoparticles (Nanoparticle Biochem, Inc) for *S. aureus* reference strain at 25 μg mL^{-1}. This value was very close to the MBC values for AgNPs obtained from the extract of *D. indica* tissues after microwave synthesis (21.2 μg mL^{-1}). The MBC values of nanoparticles synthesized from *D. indica* extract and water bath (170 μg mL^{-1}) were 8 times higher than the microwave synthesized AgNPs (21.2 μg mL^{-1}). Khan et al. (2016) found that MBC of AgNPs obtained from the *Zizipus nummularia* leaf extract was 130 μg mL^{-1}, which is more than the MBC value of any AgNPs obtained in our experiment. Sheikholeslami et al. (2016) determined the MBC value of synthetic silver nanoparticles (NanoLotus Pasargad, Inc) against *P. aeruginosa* to be 31.25 μg mL^{-1}. Brown et al. (2012), synthesized silver nanoparticles with the use of sodium borohydrate and determined their MBC value at 4 μg mL^{-1}.

We observed that G (−) plant pathogenic bacteria (*P. atrosepticum, P. parmentieri* and *D. dadantii*) were more sensitive to AgNPs in comparison to Gram negative *P. aeruginosa*. This may be related to the fact that plant pathogens have not been subjected to antibiotic pressure for millennia as compared to human pathogens. Certain multiresistant opportunistic species, such as *P. aeruginosa* and *Acinetobacter baumannii*, can colonize niches where many other species cannot survive e.g. environments with high concentration of antimicrobial agents (Beceiro et al., 2013). In addition, many of clinical isolates of *P. aeruginosa* appear to carry the impermeability type of resistance to various antibiotics (Wang et al., 2003). During our study we compared the activity of our nanoparticles to standard antibiotics. We found that in most cases AgNPs were more effective than streptomycin, but less effective than cefotaxime (Table 2). Streptomycin and copper-containing chemicals are the most frequently used for control of plant pathogenic bacteria (Kamysz et al., 2005).

What is more, the addition of carnivorous plant extracts to AgNPs can lower the needed MBC/MFC concentration. Using a checkerboard titration method in our previous study (Krychowiak et al., 2014) we found that the synergistic effect between nanoparticles and plant extracts can drastically (over 50%) lower the effective dose of this antimicrobial agents.

We have compared the activity of our nanoparticles with commercially available nanoparticles (Table 2). AgNPs from NanoAmor synthesized using chemical reduction method did not show activity towards either human or plant pathogens. Nanoparticles with surface modification (HS-(CH2)10-COOH ligand) from Prochimia Surfaces Sp. z o.o. showed activity that was comparable to AgNPs synthesized in *D. muscipula extract* with the assistance of microwave. Because our approach is a one-pot method with *in situ* derivatization, it delivers more cost effective way of AgNPs synthesis and modification.

5. Conclusions

We present a AgNPs synthesis method that uses aqueous extracts from four carnivorous plant species: *D. muscipula*, *D. binata, D. spatulata* and *D. indica*. Our research demonstrates that AgNPs synthesis with the use of biological reduction methods may be a good alternative to AgNPs synthesized with the use of synthetic reducing agents (expensive, harmful to the environment). The obtained nanoparticles were proven to be effective against human (*S. aureus*, *P. aeruginosa, C. albicans*) and plant pathogens (*P. atrosepticum, P. parmentieri* and *D. dadantii*).

Competing interest

The authors declare that they have no competing interests.

Acknowledgement

This work was financed by DS 530-M035-D673-17.

Appendix A. Supplementary material

Supplementary data associated with this article can be found, in the online version, at https://doi.org/10.1016/j.arabjc.2017.11.013.

References

Abdelwahab, S.I., Mariod, A.A., Taha, M.M.E., Zaman, F.Q., Abdelmageed, A.H.A., Khamis, S., Sivasothy, Y., Awang, K., 2017. Chemical composition and antioxidant properties of the essential oil of *Cinnamomum altissimum* Kosterm. (Lauraceae). Arab. J. Chem. 10, 131–135.

Anastas, P.T., Warner, J.C., 1998. Green Chemistry: Theory and Practice. Oxford University Press, New York, p. 30.

Ansari, M.A., Khan, H.M., Khan, A.A., Malik, A., Sultan, A., Shahid, M., Shujatullah, F., Azam, A., 2011. Evaluation of antibacterial activity of silver nanoparticles against MSSA and MRSA on isolates from skin infections. Biol. Med. 3, 141–146.

Astruc, D., Lu, F., Aranzaes, J.R., 2005. Nanoparticles as recyclable catalysts: The frontier between homogeneous and heterogeneous catalysis. Angewandte Chemie – Int. Edition, 44(48), 7852–7872.

Banasiuk, R., Frackowiak, J.E., Krychowiak, M., Matuszewska, M., Kawiak, A., Ziabka, M., Lendzion-Bielun, Z., Narajczyk, M., Krolicka, A., 2016. Synthesis of antimicrobial silver nanoparticles through a photomediated reaction in an aqueous environment. Int. J. Nanomed. 11, 315–324.

Beer, Ch., Foldbjerg, R., Hayashi, Y., Sutherland, D.S., Autrup, H., 2012. Toxicity of silver nanoparticles–nanoparticle or silver ion? Toxicol. Lett. 208 (3), 286–292.

Behrman, E.J., Kiser, R.L., Garas, W.F., Behrman, E.C., Pitt, B.M., 1995. Conversion of 4-quinolones into 3-hydroxy-4-quinolones via the corresponding sulfates. J. Chem. Res. Synop. 5, 1051–1063.

Bilecka, I., Niederberger, M., 2010. Microwave chemistry for inorganic nanomaterials synthesis. Nanoscale 2 (8), 1269–1528.

Beceiro, A., Tomás, M., Bou, G., 2013. Antimicrobial resistance and virulence: a successful or deleterious association in the bacterial world? Clin. Microbiol. Rev. 26 (2), 185–230.

Brown, A.N., Smith, K., Samuels, T.A., Lu, J., Obare, S.O., Scotta, M.E., 2012. Nanoparticles functionalized with ampicillin destroy multiple-antibiotic-resistant isolates of *Pseudomonas aeruginosa* and *Enterobacter aerogenes* and Methicillin-Resistant *Staphylococcus aureus*. Appl. Env. Microbiol. 78, 2768–2774.

Cropek, D., Kemme, P.A., Makarova, O.V., Chen, L.X., Rajh, T., 2008. Selective photocatalytic decomposition of nitrobenzene using surface modified TiO2 nanoparticles. J. Phys. Chem. C 112 (22), 8311–8318.

Dakal, T.C., Kumar, A., Majumdar, R.S., Yadav, V., 2016. Mechanistic basis of antimicrobial actions of silver nanoparticles. Front Microbiol. 7, 1831.

Duthie, E.S., Lorenz, L.L., 1952. Staphylococcal coagulase: mode of action and antigenicity. J. General Microbiol. 6, 95–107.

Eckhardt, S., Brunetto, P.S., Gagnon, J., Priebe, M., Giese, B., Fromm, K.M., 2013. Nanobio silver: its interactions with peptides and bacteria, and its uses in medicine. Chem. Rev. 113 (7), 4708–4754.

Edelstein, R.L., Tamanaha, C.R., Sheehan, P.E., Miller, M.M., Baselt, D.R., Whitman, L.J., Colton, R.J., 2000. The BARC biosensor applied to the detection of biological warfare agents. Biosensor Bioelectron. 14 (10–11), 805–813.

Finnie, J.F., van Staden, J., 1993. XII Drosera spp. (Sundew): Micropropagation and the in vitro production of plumbagin. In: Biotechnology and Agriculture and Forestry 24. Medicinal and Aromatic Plants V. Bajaj, Y.P.S., Springer – Verlag, Berlin, Heidelberg, New York, London, Paris, Tokyo, Hong Kong, Barcelona, Budapest.

Foldbjerg, R., Dang, D.A., Autrup, H., 2011. Cytotoxicity and genotoxicity of silver nanoparticles in the human lung cancer cell line, A549. Arch. Toxicol. 85 (7), 743–750.

Gurunathan, S., Kalishwaralal, K., Vaidyanathan, R., Deepak, V., Pandian, S.R.K., Muniyandi, J., Hariharan, N., Eom, S.H., 2009. Biosynthesis, purification and characterization of silver nanoparticles using Escherichia coli. Colloids Surfaces B: Biointerfaces 74, 328–335.

Juniper, B.E., Robins, R.J., Joel, D.M., 1989. Phytochemical aspects. In: The Carnivorous Plants. Harcourt Brace Jovanovich, Academic Press, London 1989, 224–240.

Kamysz, W., Krolicka, A., Bogucka, K., Ossowski, T., Lukasiak, J., Lojkowska, E., 2005. Antibacterial activity of synthetic peptides against plant pathogenic *Pectobacterium* species. J. Phytopathol. 153, 313–317.

Khan, F.A., Zahoor, M., Jalal, A., Rahman, A.U., 2016. Green synthesis of silver nanoparticles by using *Ziziphus nummularia* leaves aqueous extract and their biological activities. J. Nanomaterials, 1–8.

Khalil, M.M.H., Ismail, E.H., EI-Baghdady, K.Z., Mohamed, D., 2014. Green synthesis of silver nanoparticles using olive leaf extract and its antibacterial activity. Arab. J. Chem. 7, 1131–1139.

Kim, D., Jeong, S., Moon, J., 2006. Synthesis of silver nanoparticles using the polyol process and the influence of precursor injection. Nanotechnology 17 (16), 4019–4024.

Kittler, S., Greulich, C., Diendorf, J., Kőller, M., Epple, M., 2010. Toxicity of silver nanoparticles increases during storage because of slow dissolution under release of silver ions. Chem. Mater. 22 (16), 4548–4554.

Kreher, B., Nesmélyi, A., Wagner, H., 1990. Naphthoquinones from *Dionaea muscipula*. Phytochemistry 29, 605–606.

Krolicka, A., Szpitter, A., Gilgenast, E., Romanik, G., Kaminski, M., Lojkowska, E., 2008. Stimulation of antibacterial naphthoquinones and flavonoids accumulation in carnivorous plants by addition of elicitors. Enzyme Microb. Technol. 42, 216–221.

Krolicka, A., Szpitter, A., Maciąg, M., Biskup, E., Gilgenast, E., Romanik, G., Kaminski, M., Węgrzyn, G., Lojkowska, E., 2009. Antibacterial and antioxidant activity of the secondary metabolites from *in vitro* cultures of the Alice Sundew (*Drosera alicie*). Biotechnol. Appl. Biochem. 53, 157–184.

Krolicka, A., Szpitter, A., Stawujak, K., Baranski, R., Gwizdek-Wisniewska, A., Skrzypczak, A., Kaminski, M., Lojkowska, E., 2010. Teratomas of *Drosera capensis* var. *alba* as a source of naphthoquinone: ramentaceone. Plant Cell Tiss. Organ Cult. 103, 285–292.

Krychowiak, M., Grinholc, M., Banasiuk, R., Krauze-Baranowska, M., Glod, D., Kawiak, A., Krolicka, A., 2014. Combination of silver nanoparticles and *Drosera binata* extract as a possible alternative for antibiotic treatment of burn wound infections caused by resistant *Staphylococcus aureus*. PLOS ONE 9 (12), e115727.

Lara, H.H., Garza-Treviño, E.N., Ixtepan-Turrent, L., Singh, D.H., 2011. Silver nanoparticles are broad-spectrum bactericidal and virucidal compounds. J. Nanobiotechnol. 9, 30.

Lee, Y., Choi, J., Lee, K.J., Stott, N.E., Kim, D., 2008. Large-scale synthesis of copper nanoparticles by chemically controlled reduction for applications of inkjet-printed electronics. Nanotechnology 19 (41), 415604.

Li, S., Shen, Y., Xie, A., Yu, X., Qiu, L., Zhang, L., Zhang, Q., 2007. Green synthesis of silver nanoparticles using *Capsicum annuum* L. extract. Green Chem. 9 (8), 852–858.

Liu, J., Zhang, X., Yu, M., Li, S., Zhang, J., 2012. Photoinduced Silver Nanoparticles/Nanorings on Plasmid DNA Scaffolds. Small 8 (2), 310.

Loo, Y.Y., Chieng, B.W., Nishibuchi, M., Radu, S., 2012. Synthesis of silver nanoparticles by using tea leaf extract from *Camellia sinensis*. Int. J. Nanomedicine 7, 4263–4267.

Lubick, N., 2008. Nanosilver toxicity: ions, nanoparticles or both? Env. Sci. Technol. 42 (23). 8617 8617.

Mohapatra, B., Kuriakose, S., Mohapatra, S., 2015. Rapid green synthesis of silver nanoparticles and nanorods using *Piper nigrum* extract. J. Alloys Compd. 637, 119–126.

Morones, J.R., Elechiguerra, J.L., Camacho, A., Holt, K., Kouri, J.B., Ramírez, J.T., Yacaman, M.J., 2005. The bactericidal effect of silver nanoparticles. Nanotechnology 16, 2346–2353.

Murashige, T., Skoog, F., 1962. A revised medium for rapid growth and bioassays with tobacco tissue cultures. Plant Physiol. 15, 473–497.

Nadagouda, M.N., Speth, T.F., Varma, R.S., 2011. Microwave-assisted green synthesis of silver nanostructures. Accounts Chem. Res. 44 (7), 469–478.

Okafor, F., Janen, A., Kukhtareva, T., Edwards, V., Curley, M., 2013. Green synthesis of silver nanoparticles, their characterization, application and antibacterial activity. Int. J. Environ. Res. Public Health 10, 5221–5238.

Pal, S., Tak, Y.K., Song, J.M., 2007. Does the antibacterial activity of silver nanoparticles depend on the shape of the nanoparticle? A study of the gram-negative bacterium *Escherichia coli*. Appl. Environ. Microbiol. 73 (6), 1712–1720.

Prathna, T.C., Chandrasekaran, N., Raichur, A.M., Mukherjee, A., 2011. Biomimetic synthesis of silver nanoparticles by *Citrus limon* (lemon) aqueous extract and theoretical prediction of particle size. Colloids Surf. B Biointerfaces 82 (1), 152–159.

Prieto, P., Nistor, V., Nouneh, K., Oyama, M., Abd-Lefdil, M., Díaz, R., 2012. XPS study of silver, nickel and bimetallic silver-nickel nanoparticles prepared by seed-mediated growth. Appl. Surf. Sci. 258, 8807–8813.

Ramstedt, M., Franklyn, P., 2010. Difficulties in determining valence for Ag 0 nanoparticles using XPS – characterization of nanoparticles inside poly (3-sulphopropyl methacrylate) brushes †. 42, 855–858.

Rai, M.K., Deshmukh, S.D., Ingle, A.P., Gade, A.K., 2012. Silver nanoparticles: the powerful nanoweapon against multidrug-resistant bacteria. J. Appl. Microbiol. 112, 841–852.

Ramphal, R., Balloy, V., Jyot, J., Verma, A., Si-Tahar, M., Chignard, M., 2008. Control of *Pseudomonas aeruginosa* in the lung requires the recognition of either lipopolysaccharide or flagellin. J. Immunol. 181, 586–592.

Razzakova, D.M., Bessonova, I.A., Yunusov, S.Y., 1973. Alkaloids of *Haplophyllum acutifolium*. Khimiya Prirodnykh Soedinenii [Chemistry of Natural Compounds] 2, 206–210.

Rónavári, A., Kovács, D., Igaz, N., Vágvölgyi, C., Boros, I.M., Kónya, Z., Pfeiffer, I., Kiricsi, M., 2017. Biological activity of green-synthesized silver nanoparticles depends on the applied natural extracts: a comprehensive study. Int. J. Nanomed. 12, 871–883.

Sheikholeslami, S., Mousavi, S.E., Ashtiani, H.R.A., Doust, S.R.H., Rezayat, S.M., 2016. Antibacterial activity of silver nanoparticles and their combination with *Zataria multiflora* essential oil and methanol extract. Jundishapur J. Microbiol. 9, 1–6.

Singh, S.B., Barrett, J.F., 2006. Empirical antibacterial drug discovery–foundation in natural products. Biochem. Pharmacol. 71, 1006–1015.

Szpitter, A., Narajczyk, M., Maciag-Dorszynska, M., Wegrzyn, G., Lojkowska, E., Krolicka, A., 2014. Effect of *Dionaea muscipula* extract and plumbagin on maceration of potato tissue by *Pectobacterium atrosepticum*. Ann. Appl. Biol. 164, 404–414.

Taraszkiewicz, A., Jafra S, Skrzypczak, A., Kaminski, M., Krolicka, A., 2012. Antibacterial activity of secondary metabolites from in vitro culture of Drosera gigantea against plant patogen Pseudomonas syringae pv. syringae and P. syringae pv. morsprunorum. J. Plant Pathol. 94 (1, Suppl), 6–68.

Tran, Q.H., Nguyen, V.Q., Le, A., 2013. Silver nanoparticles: Synthesis, properties, toxicology, applications and perspectives. Adv. Nat. Sci.: Nanosci. Nanotechnol. 4(3), 033001.

Wang, Y., Ha, U., Zeng, L.S., Jin, S., 2003. Regulation of membrane permeability by a two-component regulatory system in *Pseudomonas aeruginosa*. Antimicrob. Agents Chemother. 47 (1), 95–101.

Qin, Y., Ji, X., Jing, J., Liu, H., Wu, H., Yang, W., 2010. Size control over spherical silver nanoparticles by ascorbic acid reduction. Colloids Surfaces A: Physicochem. Eng. Aspects 372, 172–176.

Zhang, X.F., Liu, Z.G., Shen, W., Gurunathan, S., 2016. Silver nanoparticles: synthesis, characterization, properties, applications, and therapeutic approaches. Int. J. Mol. Sci. 17, 1–34.